

Composite iterative learning controller design for gradually varying references with applications in an AFM system

FANG Yong-chun(方勇纯), ZHANG Yu-dong(张玉东), DONG Xiao-kun(董晓坤)

Institute of Robotics and Automatic Information System, Nankai University, Tianjin 300071, China

© Central South University Press and Springer-Verlag Berlin Heidelberg 2014

Abstract: Learning control for gradually varying references in iteration domain was considered in this research, and a composite iterative learning control strategy was proposed to enable a plant to track unknown iteration-dependent trajectories. Specifically, by decoupling the current reference into the desired trajectory of the last trial and a disturbance signal with small magnitude, the learning and feedback parts were designed respectively to ensure fine tracking performance. After some theoretical analysis, the judging condition on whether the composite iterative learning control approach achieves better control results than pure feedback control was obtained for varying references. The convergence property of the closed-loop system was rigorously studied and the saturation problem was also addressed in the controller. The designed composite iterative learning control strategy is successfully employed in an atomic force microscope system, with both simulation and experimental results clearly demonstrating its superior performance.

Key words: iterative learning control; saturation; feedback control; feedforward control; atomic force microscope

1 Introduction

Due to the merits of few system requirements and perfect tracking performance, iterative learning control (ILC) has attracted much attention in the field of control theory and applications. It was firstly proposed by ARIMOTO et al in 1984 [1] and some years later, more efforts were devoted to the research of the stability (i.e., convergence) and the transient property (convergence rate) of learning control systems. As a result, some modern control strategies were migrated into the ILC control structure to achieve better performance [2] for different systems. However, as known, in practical applications, the control system is usually perturbed by some disturbances and many uncertainties existed in the models, these factors thereby destroy the achieved convergence properties. Furthermore, the sensor noise as well as the variance in the actuating signal can also affect the final control performance. Therefore, it is quite necessary to study the robustness of ILC algorithms. According to the forms appearing in the system, the uncertainties and disturbances are categorized into two types of iteration-independent and iteration-dependent. For the former case, it needs to consider the problem of

how to design ILC algorithms to reach the desired performance as far as possible. Actually, more efforts have been devoted to the latter case. Firstly, researchers discussed the robustness of some classical ILC learning laws, such as proportional-integral-derivative (PID)-type, forgetting factor based learning laws, and Q filter tuning algorithms. Additionally, to further strengthen the defending ability against system uncertainty and unknown disturbances, some conventional robust control techniques have been employed in the ILC control architecture, such as H_∞ controller in iteration domain [3–4], wavelet-based iterative learning control [5] and optimal stochastic ILC framework [6].

However, in most of previous works, some pre-conditions, such as the assumption that the disturbance converges to zero in the iteration domain, are essentially required to ensure that the control input goes to the ideal one and the tracking error converges to zero asymptotically. Otherwise, if the disturbance is practically bounded, the tracking error can be only proven to converge into a bounded range. It should be noted that the desired trajectory is constant among trials and a premise design principle of the existing methods is to suppress the effect of the non-repeated disturbance. Nevertheless, the desired trajectories are varying along

the iteration axis. Considering this problem, we focus on the tracking problem of slowly varying references in servo systems. Under this situation, the difference of the desired trajectories between adjacent trials is small, but it becomes much more obvious after several trials. In this case, the convergence property of the existing ILC algorithms cannot be guaranteed. On the other hand, the current reference can be split into two parts consisting of the reference of last trial and some small disturbances, which leads to different ideal inputs for each trial and brings additional challenges for convergence analysis. In the literature, SAAB et al [7] first discussed this problem under the assumption that the varying trajectories are known or can be measured online. In Ref. [8], the authors proposed a new parameter adaptive law for different tracking tasks. By using internal model principle, the higher order learning algorithms are proven to be effective to deal with iteratively varying reference trajectory in Refs. [9–10].

Unfortunately, in the aforementioned researches, the varying reference trajectory or its pattern is required to be exactly known, which is too rigorous for practical systems, especially for many servo systems. Actually, we consider this problem from the application background of an atomic force microscope (AFM) system [11–13]. Under the raster scan mode of an AFM imaging system, a small tip is scanning over a preset sample line by line, while a controller is used to keep the tip-sample distance constant [14–15]. Therefore, in this system, the actuator should follow the unknown sample topography with high speed and good positioning precision [16]. However, there usually exists little variance between lines of the sample, hence it can be regarded as one of learning control systems discussed in the previous paragraph. Indeed, the idea of employing the information of last line to improve the tracking performance was first presented in Ref. [17]. Unfortunately, the previous control input is only utilized as a feedforward part without any theoretical analysis on whether it plays a positive role to enhance system performance. To utilize the previous information sufficiently, a feedforward ILC controller was designed [18], and it was combined with a feedback controller to reduce the tracking error. However, the convergence condition is derived under the assumption that the sample disturbance is invariable during trials. Though some experimental results of scanning the same line repetitively are obtained, the performance of scanning an overall image is not so good as expected. In addition, due to the limited range of the sensor measurement, the output saturation may occur in AFM systems [19]. Thus, it is also desired to study the ILC controller design approach with input/output saturation.

In this research, after summarizing the system

characteristics, a composite iterative learning control (CILC) algorithm was proposed for iteratively varying reference trajectory, and then H_∞ optimization method was employed [20] to realize the control algorithm for an AFM system. After some rigorous study, the largest variance between adjacent iterations to ensure the positive effect of the learning part was obtained in the sense of L_2 norm. Moreover, the L_2 norm of the tracking error is proven to converge into an acceptable region. Additionally, the output saturation is strictly considered in the design process of the proposed CILC scheme. Finally, the algorithms are implemented on an AFM system. Both simulation and experimental results show that the proposed CILC algorithm performs much better than the currently utilized conventional proportional-integral (PI) control law, thus, it is very promising to enhance the AFM imaging performance remarkably.

2 Problem formulation

Consider the following single-input-single-output (SISO) linear system:

$$Y(s) = G(s)U(s) \quad (1)$$

where $Y(s)$ and $U(s)$ are the Laplace transforms of the system output $y(t) \in \mathbf{R}$ and input $u(t) \in \mathbf{R}$, respectively, while $G(s)$ represents the system transfer function. The control objective for system (1) is to ensure that the output $y(t)$ tracks the iteration-dependent desired trajectory $y_{r,k}(t)$, $k = 1, 2, \dots$, in a specific time interval $t \in [0, T]$. Since the desired trajectories are assumed to be unknown and slowly varying in the iteration domain, the difference $d_{k+1}(t) \in \mathbf{R}$ between adjacent iterations is defined as

$$d_{k+1}(t) = y_{r,k+1}(t) - y_{r,k}(t) \quad (2)$$

It will be further utilized in the subsequent controller design. It is significant to point out that, the variance of references between neighboring trials is comparatively small. However, the desired signal becomes much different after a number of operations. Therefore, different from the traditional ILC systems disturbed by some iteration varying uncertainties, there is no uniform desired input which regulates the tracking error around the equilibrium point for all iterations.

To facilitate the iterative learning controller design in frequency domain, the following norms for transfer functions and signals are defined, which will be further utilized in the convergence analysis. Firstly, the L_2 norm of the signal $f(t) \in \mathbf{R}$, $t \in [0, T]$ is expressed as

$$\|f(t)\|_{L_2} = \left(\int_0^T (f(\tau))^2 d\tau \right)^{1/2}$$

In addition, the H_∞ norm of transfer function $T(s)$ is defined as

$$\|T(s)\|_\infty = \sup_{\omega} \{T(j\omega)\}$$

Considering the fact that the transfer function H_∞ norm is the induced norm corresponding to the L_2 norm for signals, the following result will be employed in the subsequent analysis. If $x_2(t) = T(s)x_1(t)$, $x_1(t) \in \mathbf{R}$, $x_2(t) \in \mathbf{R}$, then

$$\|x_2(t)\|_{L_2} \leq \|T(s)\|_\infty \|x_1(t)\|_{L_2} \quad (3)$$

In addition, to describe the signal transmission explicitly, all the signals are expressed in the time domain, with the only exception that the transfer functions are defined in frequency domain.

3 Composite iterative learning controller design

To achieve the above control goal, the composite iterative learning control strategy combining feedback and feedforward terms is proposed as shown in Fig. 1, where $C_{FF}(s)$ and $C_{FB}(s)$ are the feedforward learning control law and feedback controller, respectively. For the iteration indexed as number $(k+1)$, the system output and control error are expressed as $y_{k+1}(t)$ and $e_{k+1}(t)$, respectively.

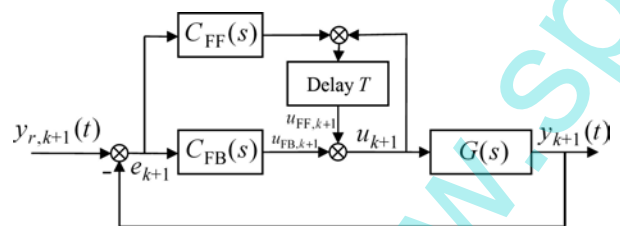


Fig. 1 Control block diagram of designed CILC scheme

The control input $u_{k+1}(t)$ of the $(k+1)$ -th trial is composed of two parts:

$$u_{k+1}(t) = u_{FB,k+1}(t) + u_{FF,k+1}(t) \quad (4)$$

with the feedforward learning controller as

$$u_{FF,k+1}(t) = u_k(t) + C_{FF}e_k(t) \quad (5)$$

To complete the control objective, the following design criteria are proposed to design the feedforward and feedback parts:

- 1) This composite controller can achieve better performance than that of pure feedback or feedforward algorithm;
- 2) The L_2 norm of the controlled error can finally converge into an acceptable region;
- 3) When the reference is not varying with iterations, the L_2 norm of the error can converge to zero

monotonically;

- 4) When the measured output is saturated due to the sensor measurement range, the previous properties still hold.

According to the above principles, the subsequent subsections carefully study the performance of this CILC scheme as well as its convergence property and implementation technique.

3.1 Comparison with case of pure feedback or feedforward control

The references of the learning control system are varying with iterations, hence it is essential to study whether the learning term plays a positive role or not in the closed-loop system. In this subsection, the comparison between the proposed composite control mode and the individual feedforward/feedback part is discussed, and a guideline whether using the CILC controller or not is presented subsequently. To achieve this goal, the control error under the proposed algorithm with iteration number of $(k+1)$ is expressed as $e_{k+1}(t) \in \mathbf{R}$ and

$$\begin{aligned} e_{k+1}(t) &= y_{r,k+1}(t) - y_{k+1}(t) = y_{r,k+1}(t) - \\ &\frac{GC_{FB}}{1+GC_{FB}}y_{r,k+1}(t) - \frac{G}{1+GC_{FB}}u_{FF,k+1}(t) = \\ &\frac{1}{1+GC_{FB}}(y_{r,k}(t) + d_{k+1}(t)) - \\ &\frac{G}{1+GC_{FB}}(u_k(t) + C_{FF}e_k(t)) = \\ &\frac{1}{1+GC_{FB}}(y_{r,k}(t) - Gu_k(t)) - \frac{GC_{FF}}{1+GC_{FB}}e_k(t) + \\ &\frac{1}{1+GC_{FB}}d_{k+1}(t) = \frac{1-GC_{FF}}{1+GC_{FB}}e_k(t) + \\ &\frac{1}{1+GC_{FB}}d_{k+1}(t) \end{aligned} \quad (6)$$

In addition, the control errors of individual feedback and feedforward strategy are described as $e'_{k+1}(t) \in \mathbf{R}$ and $e''_{k+1}(t) \in \mathbf{R}$, respectively

$$e'_{k+1}(t) = \frac{1}{1+GC_{FB}}y_{r,k+1}(t) = \frac{1}{1+GC_{FB}}(y_{r,k}(t) + d_{k+1}(t)) \quad (7)$$

$$\begin{aligned} e''_{k+1}(t) &= y_{r,k+1}(t) - y_{k+1}(t) = \\ &y_{r,k+1}(t) - Gu_{FF,k+1}(t) = \\ &(y_{r,k}(t) + d_{k+1}(t)) - G(u_k(t) + C_{FF}e_k(t)) = \\ &(y_{r,k}(t) - Gu_k(t)) - GC_{FF}e_k(t) + d_{k+1}(t) = \\ &(1-GC_{FF})e_k(t) + d_{k+1}(t) \end{aligned} \quad (8)$$

The following theorem is presented to describe the

superiority of the CILC over the other two methods as well as the necessary condition for the variance of iteration-dependant references.

Theorem 1: For the learning control system Eq. (1) with varied references Eq. (2), if the control law Eq. (4) and the reference variance satisfy these conditions:

$$\begin{cases} \left\| \frac{1}{1+GC_{FB}} \right\|_{\infty} \leq 1 \\ 1 - \|L(s)\|_{\infty} \geq 2 \frac{\|d_{k+1}(t)/(1+GC_{FB})\|_{l_2}}{\|y_{r,k}(t)/(1+GC_{FB})\|_{l_2}} \\ \left\| \frac{d_{k+1}(t)}{1+GC_{FB}} \right\|_{l_2} \leq \frac{1}{2} \left\| \frac{y_{r,k}(t)}{1+GC_{FB}} \right\|_{l_2} \end{cases} \quad (9)$$

where $L(s) = (1 - GC_{FF}) / (1 + GC_{FB})$ denotes the error transfer function in iteration domain, and $d_{k+1}(t)$ is defined in Eq. (2), then the control performance of the composite ILC controller is better than that of only feedback or feedforward control in the sense:

$$\begin{cases} \|e_{k+1}(t)\|_{l_2} \leq \|e'_{k+1}(t)\|_{l_2} \\ \|e_{k+1}(t)\|_{l_2} \leq \|e''_{k+1}(t)\|_{l_2} \end{cases} \quad (10)$$

Proof: To prove **Theorem 1**, firstly express the L_2 norm of the $(k+1)$ -th trial tracking error as

$$\|e_{k+1}(t)\|_{l_2} = \left\| L(s)e_k(t) + \frac{1}{1+GC_{FB}}d_{k+1} \right\|_{l_2} \quad (11)$$

Moreover, utilizing the result of inequation (3) and the condition of inequation (9) yields

$$\begin{aligned} \|e_{k+1}(t)\|_{l_2} &\leq \|L(s)\|_{\infty} \|e_k(t)\|_{l_2} + \left\| \frac{d_{k+1}(t)}{1+GC_{FB}} \right\|_{l_2} \leq \\ &\left(1 - 2 \frac{\|d_{k+1}(t)/(1+GC_{FB})\|_{l_2}}{\|y_{r,k}(t)/(1+GC_{FB})\|_{l_2}} \right) \|e_k(t)\|_{l_2} + \\ &\left\| \frac{d_{k+1}(t)}{1+GC_{FB}} \right\|_{l_2} \end{aligned} \quad (12)$$

In inequation (12), if the L_2 norm of the k -th trial control error is less than that of only feedback control

$$\|e_k(t)\|_{l_2} \leq \|e'_k(t)\|_{l_2} = \left\| \frac{y_{r,k}(t)}{1+GC_{FB}} \right\|_{l_2} \quad (13)$$

then, by substituting inequation (13) into inequation (12), we have

$$\begin{aligned} \|e_{k+1}(t)\|_{l_2} &\leq \left\| \frac{y_{r,k}(t)}{1+GC_{FB}} \right\|_{l_2} - \left\| \frac{d_{k+1}(t)}{1+GC_{FB}} \right\|_{l_2} \leq \\ &\left\| \frac{y_{r,k}(t) + d_{k+1}(t)}{1+GC_{FB}} \right\|_{l_2} = \|e'_{k+1}(t)\|_{l_2} \end{aligned} \quad (14)$$

Therefore, in case of the assumption that

$$\|e_2(t)\|_{l_2} \leq \|e'_2(t)\|_{l_2} \quad (15)$$

for any $k=3, \dots$, it is straightforward to conclude that $\|e_{k+1}(t)\|_{l_2} \leq \|e'_{k+1}(t)\|_{l_2}$. To verify this assumption, $e_2(t)$ is rewritten as

$$\begin{aligned} e_2(t) &= \frac{1 - GC_{FF}}{1 + GC_{FB}} e_1(t) + \frac{1}{1 + GC_{FB}} d_2(t) = \\ &\frac{1 - GC_{FF}}{1 + GC_{FB}} \frac{1}{1 + GC_{FB}} y_{r,1}(t) + \frac{1}{1 + GC_{FB}} d_2(t) \end{aligned} \quad (16)$$

Taking the L_2 norm of Eq. (16) obtains

$$\begin{aligned} \|e_2(t)\|_{l_2} &= \left\| L(s) \frac{1}{1 + GC_{FB}} y_{r,1}(t) + \frac{1}{1 + GC_{FB}} d_2(t) \right\|_{l_2} \leq \\ &\|L(s)\|_{\infty} \left\| \frac{y_{r,1}(t)}{1 + GC_{FB}} + \frac{d_2(t)}{1 + GC_{FB}} \right\|_{l_2} \end{aligned} \quad (17)$$

By utilizing the condition in inequation (9), it gives

$$\begin{aligned} \|e_2(t)\|_{l_2} &\leq \left(1 - 2 \frac{\|d_2(t)/(1 + GC_{FB})\|_{l_2}}{\|y_{r,1}(t)/(1 + GC_{FB})\|_{l_2}} \right) \left\| \frac{y_{r,1}(t)}{1 + GC_{FB}} \right\|_{l_2} + \\ &\left\| \frac{d_2(t)}{1 + GC_{FB}} \right\|_{l_2} = \left\| \frac{y_{r,1}(t)}{1 + GC_{FB}} \right\|_{l_2} - \left\| \frac{d_2(t)}{1 + GC_{FB}} \right\|_{l_2} \leq \\ &\left\| \frac{y_{r,1}(t) + d_2(t)}{1 + GC_{FB}} \right\|_{l_2} = \|e'_2(t)\|_{l_2} \end{aligned} \quad (18)$$

It implies that the assumption inequation (15) holds.

Therefore, $\|e_k(t)\|_{l_2} \leq \|e'_k(t)\|_{l_2}$ indicates that the composite ILC strategy makes the system (1) track the varied trajectory more precisely than that of feedback control under the condition inequation (9). Furthermore, the proposed control scheme is inspected with the conventional ILC structure without feedback term. To this end, the L_2 norm of $e_{k+1}(t)$ is taken and the resulting expression is manipulated as

$$\begin{aligned} \|e_{k+1}(t)\|_{l_2} &= \left\| \frac{(1 - GC_{FF})e_k(t) + d_{k+1}(t)}{1 + GC_{FB}} \right\|_{l_2} \leq \\ &\left\| \frac{1}{1 + GC_{FB}} \right\|_{\infty} \|(1 - GC_{FF})e_k(t) + d_{k+1}(t)\|_{l_2} = \\ &\left\| \frac{1}{1 + GC_{FB}} \right\|_{\infty} \|e''_{k+1}(t)\|_{l_2} \end{aligned} \quad (19)$$

According to the condition inequation (9), we know that $\|e_{k+1}(t)\|_{l_2} \leq \|e''_{k+1}(t)\|_{l_2}$. Therefore, the control performance of the proposed CILC approach is also better than that of traditional no-feedback ILC scheme.

Theorem 1 provides a judging criterion for when the composite iterative learning controller can be employed to deal with the problem of varying references. That is, when the variance between adjacent trials is

small compared with the base references (condition inequation (9)), the proposed CILC strategy can be employed to achieve better control performance.

Remark 1: To make the condition inequation (9) hold, both the feedforward learning law $C_{FF}(s)$ and the feedback part $C_{FB}(s)$ need to be elaborately designed based on the behavior of the varying trajectory. That is, if an almost inverse controller is ideally adopted for the feedforward law $C_{FF}(s)$, then the error transfer function $L(s)$ is close to zero, which then provides much flexibility for the design of the feedback part $C_{FB}(s)$. However, as this design methodology is difficult to implement for practical systems, suitable feedforward term $C_{FF}(s)$ is usually proposed to compensate for the dynamics of the $G(s)$ at interested frequency region.

3.2 Convergence analysis

In this subsection, the convergence property of the proposed CILC strategy is studied. And the following theorem is suggested to present the convergent performance.

Theorem 2: If the control system Eq. (1) satisfies:

- 1) The control law consisting of C_{FF} and C_{FB} is designed in accordance with inequation (9);
- 2) The L_2 norm of the variance between adjacent references is bounded by a small positive constant $\varepsilon \in \mathbf{R}^+$, that is

$$\forall k = 2, \dots, \|d_k(t)\|_{L_2} \leq \varepsilon,$$

the learning system Eq. (1) converges in the following senses:

- 1) The tracking error in each iteration is L_2 norm bounded;
- 2) When $k \rightarrow \infty$, $\|e_k(t)\|_{L_2}$ enters into an appropriate range;
- 3) If the reference in iteration domain is constant, the tracking error decreases monotonically with iterations, and it finally converges to zero.

Proof: Firstly, the tracking errors during the first and second trials are given as

$$\begin{cases} e_1(t) = \frac{1}{1+GC_{FB}} y_{r,1}(t) \\ e_2(t) = \frac{1-GC_{FF}}{1+GC_{FB}} e_1(t) + \frac{1}{1+GC_{FB}} d_2(t) \end{cases} \quad (20)$$

Similarly, $e_k(t)$, $k = 3, 4, \dots$, are expressed as

$$e_k(t) = \left(\frac{1-GC_{FF}}{1+GC_{FB}}\right)^{k-1} e_1(t) + \left(\frac{1-GC_{FF}}{1+GC_{FB}}\right)^{k-2} \times \frac{1}{1+GC_{FB}} d_2(t) + \dots + \frac{1}{1+GC_{FB}} d_k(t) \quad (21)$$

Taking the L_2 norm of Eq. (21) yields

$$\begin{aligned} \|e_k(t)\|_{L_2} &\leq \|L(s)\|_{\infty}^{k-1} \|e_1(t)\|_{L_2} + \\ &\|L(s)\|_{\infty}^{k-2} \left\| \frac{1}{1+GC_{FB}} \right\|_{\infty} \|d_2(t)\|_{L_2} + \dots + \\ &\left\| \frac{1}{1+GC_{FB}} \right\|_{\infty} \|d_2(t)\|_{L_2} \leq \|L(s)\|_{\infty}^{k-1} \|e_1(t)\|_{L_2} + \\ &(\|L(s)\|_{\infty}^{k-2} + \dots + 1) \left\| \frac{1}{1+GC_{FB}} \right\|_{\infty} \varepsilon = \\ &\|L(s)\|_{\infty}^{k-1} \|e_1(t)\|_{L_2} + \frac{1}{1-\|L(s)\|_{\infty}} \left\| \frac{1}{1+GC_{FB}} \right\|_{\infty} \varepsilon \quad (22) \end{aligned}$$

Since all the terms appeared in the above equation are bounded, $\|e_k(t)\|_{L_2}$ is also bounded. Furthermore, when $k \rightarrow \infty$,

$$\|e_k(t)\|_{L_2} \leq \frac{1}{1-\|L(s)\|_{\infty}} \left\| \frac{1}{1+GC_{FB}} \right\|_{\infty} \varepsilon \quad (23)$$

Thus, with increasing iteration number, the tracking error gradually enters into the range given in inequation (23). It should be noted that when the desired output is iteration-independent which implies that $\varepsilon=0$, then inequation (22) is rewritten as

$$\|e_k(t)\|_{L_2} \leq \|L(s)\|_{\infty}^{k-1} \|e_1(t)\|_{L_2} \quad (24)$$

In this case, the tracking error converges to zero monotonically in the sense of L_2 norm.

3.3 Study for output saturation problem

As stated in the introduction part, the control input in some situations may exceed the effective actuating range. In addition, the control error may also go beyond the sensor scope. It is named as input/output saturation. Without loss of generality, the sensor saturation is taken as an instance in this work to verify the effectiveness of the constructed CILC control law when saturation happens.

Firstly, the saturation function is defined as

$$\text{Sat}_{e_0}(e_k(t)) = \begin{cases} e_0, & e_k(t) \geq e_0 \\ e_k(t), & -e_0 < e_k(t) < e_0 \\ -e_0, & e_k(t) \leq -e_0 \end{cases} \quad (25)$$

where e_0 is a positive constant representing the maximum value that can be measured by the sensor. To facilitate the analysis in frequency domain, the saturation nonlinearity is re-expressed by the describing function as

$$N(A) = \frac{2}{\pi} \left[\arcsin \frac{e_0}{A} + \frac{e_0}{A} \sqrt{1 - \left(\frac{e_0}{A}\right)^2} \right] \quad A \geq e_0 \quad (26)$$

which approximates the saturation nonlinearity by the

first harmonic components with A denoting the amplitude of the input sine wave. Then, the tracking error is rewritten as

$$e_{k+1}(t) = y_{r,k+1}(t) - N(A)GC_{FB}e_{k+1}(t) - Gu_{FF,k+1}(t) \quad (27)$$

Further, it is arranged as

$$e_{k+1}(t) = \frac{y_{r,k+1}(t) - Gu_{FF,k+1}(t)}{1 + N(A)GC_{FB}} = \frac{y_{r,k}(t) + d_{k+1}(t) - G(u_k(t) + N(A)C_{FF}e_k(t))}{1 + N(A)GC_{FB}} = \frac{1 - N(A)GC_{FF}}{1 + N(A)GC_{FB}}e_k(t) + \frac{d_{k+1}(t)}{1 + N(A)GC_{FB}} \quad (28)$$

Since $0 < N(A) \leq 1$, $A \geq e_0$, then when saturation happens, the design principles in **Theorem 1** are used on $N(A)C_{FF}$ and $N(A)C_{FB}$ instead of C_{FF} and C_{FB} , where the amplitude of $N(A)$ depends on the prediction of the exceeding range of the tracking error over the measuring scope.

3.4 H_∞ controller synthesis

Through the previous analysis, it is known that for slowly varying references, to meet the requirements introduced in the beginning of Section 3, the design for the feedforward control C_{FF} and feedback law C_{FB} should follow these two guidelines:

$$\left\| \frac{1}{1 + N(A)GC_{FB}} \right\|_\infty \leq 1 \quad (29)$$

and

$$1 - \left\| \frac{1 - N(A)GC_{FF}}{1 + N(A)GC_{FB}} \right\|_\infty \geq \frac{2 \left\| \frac{d_{k+1}(t)/(1 + N(A)GC_{FB})}{y_{r,k}(t)/(1 + N(A)GC_{FB})} \right\|_{l_2}}{\left\| \frac{d_{k+1}(t)/(1 + N(A)GC_{FB})}{y_{r,k}(t)/(1 + N(A)GC_{FB})} \right\|_{l_2}} \quad (30)$$

According to these two items, the standard H_∞ optimization method is employed to obtain the two controllers.

1) The H_∞ norm optimal feedback controller C_{FB} can be calculated as

$$\min_{C_{FB}} \left\| \frac{(1 + N(A)GC_{FB})^{-1}W_1}{C_{FB}(1 + N(A)GC_{FB})^{-1}W_2} \right\|_\infty \quad (31)$$

where W_1 and W_2 are weight functions designed for error transfer function and control input, respectively. In actual applications, W_1 is usually designed as a low-pass filter to obtain good tracking performance under low frequency. Besides, to avoid oscillation or saturation of actuators, a small constant or the first order resonant part of the system dynamics is employed to construct W_2 .

2) Based on the feedback controller C_{FB} , the learning law C_{FF} is optimized as

$$\min_{C_{FF}} \left\| \frac{1 - N(A)GW_3C_{FF}}{1 + N(A)GC_{FB}} \right\|_\infty \quad (32)$$

where the low-pass filter W_3 is used in the optimization process to guarantee that the H_∞ norm of the error transfer function maintains at a small level in the desired frequency band. Ideally, the feedforward term C_{FF} should be chosen as the inversion of the system transfer function $G(s)$, which then makes $L(s)$ approach zero. However, due to the non-minimum phase problem which may appear in $G(s)$, H_∞ optimization method is used in this work to obtain the approximate system inversion under the premise of controller stability.

4 Simulation results

To thoroughly verify the performance of the proposed control strategy, both simulation and experiments are conducted on an atomic force microscope system, which is an important imaging tool on nanotechnology. To fully investigate the performance of the designed CILC control strategy, it is firstly compared with a standard feedback control law by some simulation tests, and then employed in a practical AFM system and the imaging results are compared with those obtained from the currently utilized proportional-integral (PI) control method.

For the simulation, the following model $G(s)$ obtained from a practical AFM platform is utilized [21]:

$$G(s) = \frac{9.75 \times 10^4 s^2 + 3.00 \times 10^7 s + 1.81 \times 10^{13}}{s^3 + 6.31 \times 10^4 s^2 + 1.84 \times 10^8 s + 1.06 \times 10^{13}} \quad (33)$$

In addition, the system measurement range is $[-0.5, 0.5]$. Based on the above model setup, the following low-pass filter W_1 is used in the H_∞ optimization process to guarantee good tracking performance as

$$W_1(s) = \frac{0.1s + 2000}{s + 2000} \quad (34)$$

Moreover, W_2 is chosen as 0.1 to suppress the magnitude of the control input. Through the calculation algorithm (31), the feedback controller is obtained by using the Matlab hinfsv function.

Let the presented control system track the following iteration-varying desired trajectories:

$$y_{r,k}(t) = 0.4 \left(\sin \left(\frac{\pi}{20} k \right) + 2 \frac{1}{j} (\sin(200\pi t) + 0.5 \sin(80\pi t)) \right), \quad k=1, 2, \dots \quad (35)$$

It is easy to see that the amplitude of this hybrid sine wave signal varies with different iterations. In the simulation, the normally distributed signal with mean of 0 and mean-square deviation of 0.1 is inserted into the system as measurement noise. Then, some comparative

tests for the proposed algorithm and the feedback control are carried out in the simulation platform.

The simulation results are shown in Figs. 2 and 3. Figure 2 depicts the tracking results during the 50th iteration. It is evident that the output with the CILC control is quite close to the reference, however, large error exists when using the feedback control. To further demonstrate the learning performance, the L_2 norm of the tracking error is calculated and plotted in Fig. 3. The results imply that the L_2 norm of the proposed algorithm is kept at small values after some iterations, which is much less than that of feedback control.

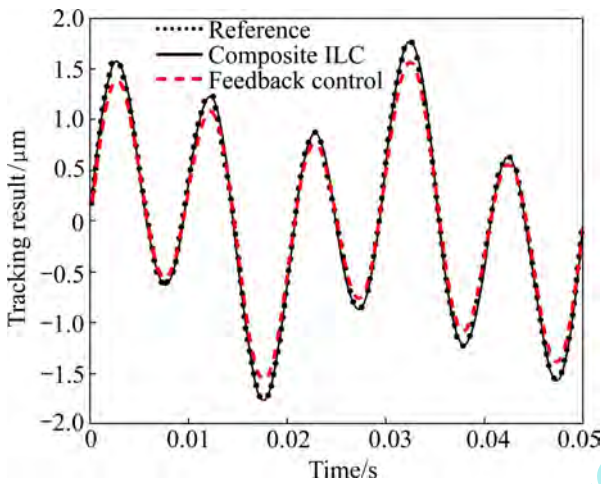


Fig. 2 Tracking result of 50th trial

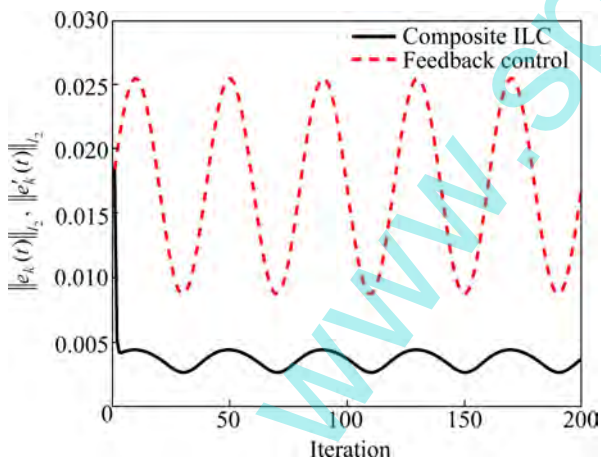


Fig. 3 $\|e_k(t)\|_{L_2}$ and $\|e'_k(t)\|_{L_2}$ in iteration domain

In addition, the relationship from time and iteration to the tracking error is expressed by 3-dimensional images, as shown in Fig. 4. Figure 4(a) shows the tracking error of the presented approach, while Fig. 4(b) shows the feedback control result. From this comparison, it is known that in most of the iteration and time domains, the former is smaller than the latter except at the beginning several iterations. From the viewpoint of the AFM operation, lower control error infers that a faster scanning speed is possible, and it effectively decreases

the interaction between the probe and the sample, which thus enhances the protection for both of them during the imaging process.

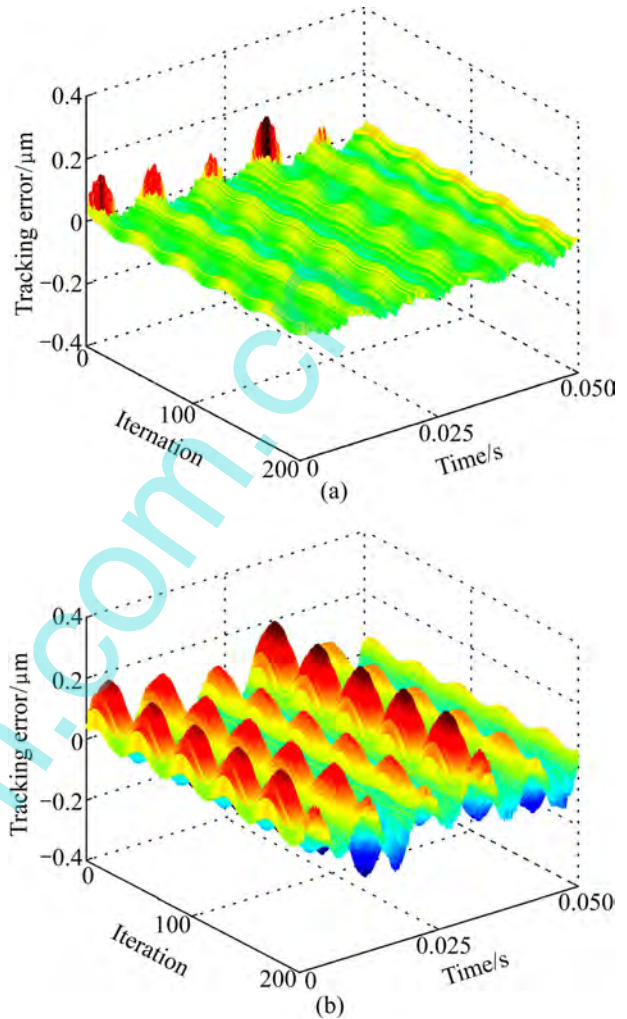


Fig. 4 3-D diagram of tracking error (a) and feed back control (b) in iteration and time domains

5 Application and analysis

After sufficient simulation test, the proposed CILC control method is applied to an atomic force microscope system and collect experimental results to further verify its effectiveness. To implement comparative study, experimental results of both the CILC controller and the currently utilized control law are provided.

As shown in Fig. 5, the lab-developed AFM control system consists of an AFM body (CSPM4000, Being NANO Ltd.), a signal processing card, and a RTLinux based controller. The basic working principle of the AFM is to maintain the deflection of the probe constant by tuning the displacement of a piezo-scanner in z -axis. Under the command of the x and y motion controllers, the probe is scanning across the surface of the sample in a raster mode. Then, by recording x and y coordinates and the control signal in z axis, the sample topography is

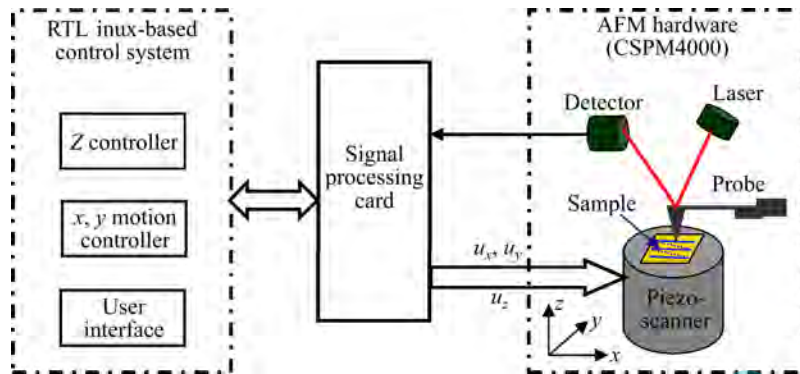


Fig. 5 Scheme of RTLinux-based atomic force microscope control system

obtained indirectly. From the viewpoint of iterative learning control, the sample surface is regarded as unknown trajectories tracked by the piezo-scanner. Since it is usually slowly time-varying and the scan is implemented line-by-line, the references are iteration-dependent and there is little difference between adjacent trials. Therefore, the proposed CILC algorithm is utilized to enable the piezo-scanner to track the sample surface when the reference voltage of the laser detector is set as a constant. In addition, when a sudden drop appears in the sample, the probe loses contact with the surface, thus, the sensor cannot observe the change of the output accurately and then saturation occurs.

Note that in current AFMs, a PI controller is employed to stabilize the piezo-scanner. Therefore, based on the above experiment setup, the proposed CILC control algorithm is compared with the currently utilized PI controller. In the experiment, a one-dimensional calibration grating (with period of 3 μm and step of 80 nm) is selected as the test sample. The other scanning parameters are set as scanning range (5 μm), image resolution (200 \times 200) and scanning frequency (10 Hz, 10 lines per second).

Firstly, the setpoint is chosen as 0.4 V. After some calculations, it is known that the surface variance of 80 nm is less than the range of the sensor measurement, thus output saturation does not exist in this test. The AFM images with the two control approaches are depicted in Fig. 6, where Fig. 6(a) shows the scanning result of the proposed CILC control, and Fig. 6(b) shows the image obtained by PI control. It is shown that the AFM image of the PI controller is blurred at the rising and trailing edges, which implies that the PI controller cannot yield satisfactory performance when the AFM scans through the selected calibration grating. To clearly demonstrate the advantages of the proposed technique, the tracking error of the 100th iteration is shown in Fig. 7. The results indicate that the designed CILC controller suppresses the regulation error remarkably.

Subsequently, it is usually required to lower the

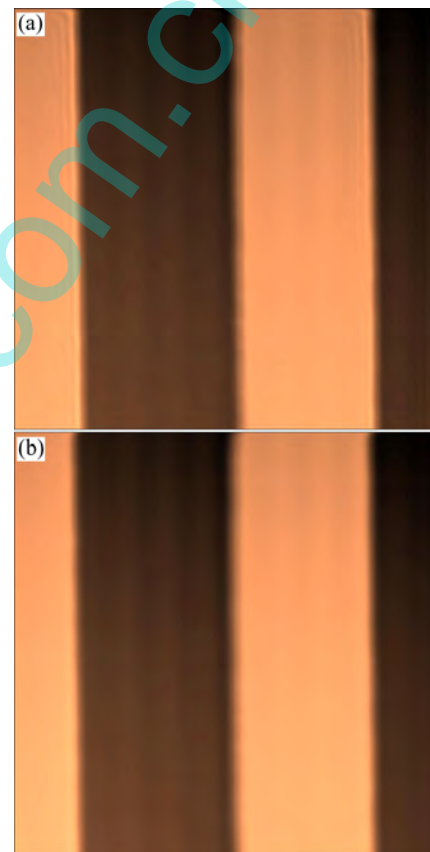


Fig. 6 AFM images of calibration grating without sensor saturation: (a) CILC law; (b) PI control

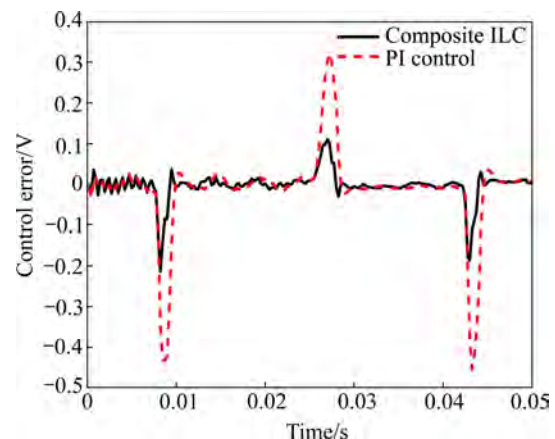


Fig. 7 Tracking error of 100th iteration without sensor saturation

setpoint of the AFM system to reduce the interaction between the probe-tip and the sample for many soft samples. Under this situation, the deflection of the micro-cantilever at setpoint is small, which then decreases the measurement range, thus the output saturation tends to happen frequently. To validate the control performance under this situation, 0.1 V is chosen as the setpoint during the scanning process. Since the output can not be negative, whenever the tracking error is less than -0.1 V, the system then enters the saturation range. Figures 8 and 9 present the experimental results with this parameter setup. By comparing Fig. 8(a) with Fig. 6(a), it can be seen that the obtained images from the CILC algorithms for both with/without saturations are similar, while for the images obtained from the PD controller, the saturation situation is much worse as the unclear edges indicated in Fig. 8(b). These results show that when output saturation occurs, the imaging performance of the PI control is degraded badly (Fig. 8(b)), while the designed CILC controller still keeps good AFM image quality (Fig. 8(a)). In addition, the control error is regulated into the measurement range with the proposed control law, however, it takes much longer time for the PI controller (see Fig. 9).

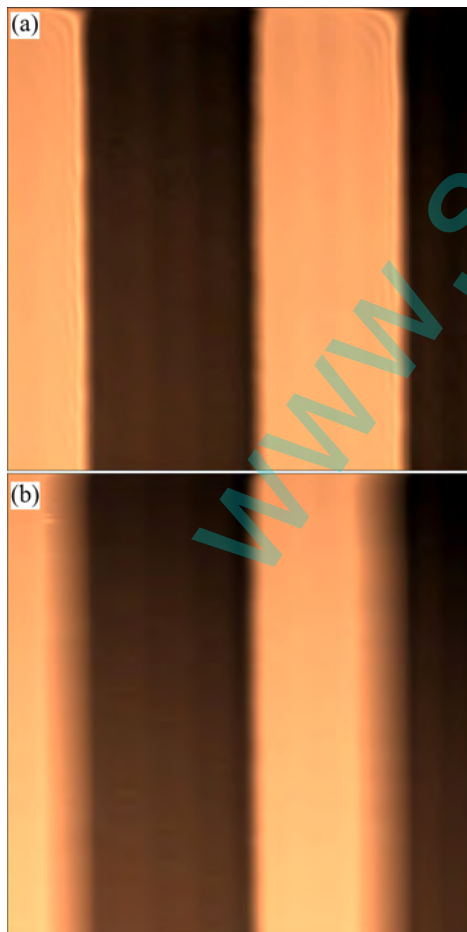


Fig. 8 AFM images of calibration grating with sensor saturation: (a) CILC law; (b) PI control

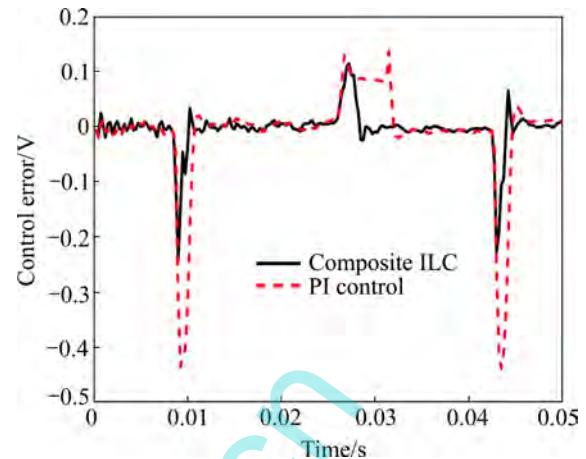


Fig. 9 Tracking error of 100th iteration with sensor saturation

5 Conclusions

1) A composite iterative learning control approach is proposed to address the tracking control problem for gradually varying references in iteration domain. The current reference is broken up into two parts of last reference and some disturbance signal, which is then respectively addressed by the feedforward learning controller and the feedback controller.

2) The presented learning controller is proven to be convergent and the case of output saturation is strictly considered during the design process. The designed CILC strategy is finally utilized in an atomic force microscope system, and both simulation and experimental results are collected to demonstrate the effectiveness of the proposed control algorithm.

References

- [1] ARIMOTO S, KAWAMURA S, MIYAZAKI F. Bettering operation of robots by learning [J]. *Journal of Robotic Systems*, 1984, 1(2): 123–140.
- [2] BRISTOW D A, THARAYIL M, ALLEYNE A G. A survey of iterative learning control [J]. *IEEE Control Systems Magazine*, 2006, 26(3): 96–114.
- [3] MOORE K L, CHEN Y, AHN H. Algebraic H_∞ design of higher-order iterative learning controllers [C]// *Proceedings of 2005 IEEE International Symposium on Intelligent Control*. Limassol, Cyprus: IEEE Press, 2005: 1213–1218.
- [4] MENG D, JIA Y, DU J, YU F. H_∞ -based design approach to discrete-time learning control systems with iteration-varying disturbances [C]// *Proceedings of 48th IEEE Conference on Decision and Control*. Shanghai, China: IEEE Press, 2009: 4882–4887.
- [5] MERRY R, MOLENGRAFT R, STEINBUCH M. Removing non-repetitive disturbances in iterative learning control by wavelet filtering [C]// *Proceedings of 2006 American Control Conference*. Minneapolis, USA: IEEE Press, 2006: 226–231.
- [6] SAAB S A. A stochastic iterative learning control algorithm with application to an induction motor [J]. *International Journal of Control*, 2004, 77(2): 144–163.
- [7] SAAB S, VOGT W G, MICKLE M H. Learning control algorithms

- for tracking “slowly” varying trajectories [J]. IEEE Transactions on Systems, Man, and Cybernetics-Part B: Cybernetics, 1997, 27(4): 657–670.
- [8] XU J X, XU J. On iterative learning from different tracking tasks in the presence of time-varying uncertainties [J]. IEEE Transactions on Systems, Man, and Cybernetics-Part B: Cybernetics, 2004, 34(1): 589–597.
- [9] CHEN Y, MOORE K L. Harnessing the nonrepetitiveness in iterative learning control [C]// Proceedings of 41st IEEE Conference on Decision and Control. Las Vegas, USA: IEEE Press, 2002: 3350–3355.
- [10] LIU C, XU J, WU J. Iterative learning control with high-order internal model for linear time-varying systems [C]// Proceedings of 2009 American Control Conference. St. Louis, USA: IEEE Press, 2009: 1634–1639.
- [11] SHIBATA M, YAMASHITA H, UCHIHASHI T, KANDORI H, ANDO T. High-speed atomic force microscopy shows dynamic molecular processes in photo-activated bacteriorhodopsin [J]. Nature Nanotechnology, 2010(5): 208–212.
- [12] SHIGETO I, TAKAYUKI U, DAISUKE Y, TOSHIO A. Direct observation of surfactant aggregate behavior on a mica surface using high-speed atomic force microscopy [J]. Chem Commun, 2011(47): 4974–976.
- [13] ONAL C D, OZCAN O, SITTI M. Automated 2-D nanoparticle manipulation using atomic force microscopy [J]. IEEE Transactions on Nanotechnology, 2011, 10(3): 472–481.
- [14] BASSO M, PAOLETTI P, TIRIBILLI B, VASSALLI M. AFM imaging via nonlinear control of self-driven cantilever oscillations [J]. IEEE Transactions on Nanotechnology, 2011, 10(3): 560–565.
- [15] ZHANG Yu-dong, FANG Yong-chun, YU Jie, DONG Xiao-kun. Note: A novel atomic force microscope fast imaging approach: Variable-speed scanning [J]. Review of Scientific Instrument, 2001, 82: 056103. 1–3.
- [16] ZHANG Yu-dong, FANG Yong-chun, ZHOU Xian-wei, DONG Xiao-kun. Image-based hysteresis modeling and compensation for an AFM piezo-scanner [J]. Asian Journal of Control, 2009, 11(2): 166–174.
- [17] SCHITTER G, STEMMER A, ALLGÖWER F. Robust two-degree-of-freedom control of an atomic force microscope [J]. Asian Journal of Control, 2004, 6(2): 156–163.
- [18] WU Y, ZOU Q, SU C. A current cycle feedback iterative learning control approach for AFM imaging [J]. IEEE Transactions on Nanotechnology, 2009, 8(4): 515–527.
- [19] ZHANG Y, FANG Y, DONG X. Output feedback robust adaptive controller design for dynamic atomic force microscopy [C]// Proceedings of IEEE Conference on Control Applications Yokohama. Japan: John Wiley & Sons, 2010: 1666–1671.
- [20] AMANN N, OWENS D H. An H_∞ approach to linear iterative learning control design [J] International Journal of Adaptive Control and Signal Processing, 1996, 10(6): 767–781.
- [21] ZHOU Xian-wei. Research on control of AFM based nano-imaging and nano-manipulation [D]. Tianjin: Nankai University, 2009.

(Edited by FANG Jing-hua)